# Positron emission tomographic studies of the cortical anatomy of single-word processing

**S. E. Petersen, P. T. Fox, M. I. Posner, M. Mintun & M. E. Raichle**

Department of Neurology and Neurological Surgery, Washington University School of Medicine, 660 South Euclid Avenue, St Louis, Missouri 63110, USA

*The use of positron emission tomography to measure regional changes in average blood flow during processing of individual auditory and visual words provides support for multiple, parallel routes between localized sensory-specific, phonological, articulatory and semantic-coding areas.*

LANGUAGE is an essential characteristic of the human species, and has been studied by disciplines ranging from philosophy to neurology. Because language is so complex, cognitive and neurological studies often focus on processing of individual words (lexical items). Cognitive models for lexical processing consider words perceived visually and auditorily to involve separate modality-specific codes, with access in parallel to shared output (articulatory) and meaning (semantic) codes[1-6]. In contrast, the model most widely accepted in the clinical neurological literature argues for serial processing, with an early recoding of visual input into an auditory-based code which is used in turn for semantic and articulatory access[7,8].

We have used recent advances in the precision of positron emission tomography (PET) for measuring activity-related changes in regional cerebral blood flow to identify brain regions active during three levels of single-word processing. Our results indicate localization of different codes in widely separated areas of the cerebral cortex. The results favour the idea of separate brain areas involved in separate visual and auditory coding of words, each with independent access to supramodal articulatory and semantic systems. These findings fit well with the parallel models, but argue against the obligatory visual-to-auditory recoding and serial nature of the clinical neurological models.

## Methods

Brain blood flow was measured in 17 (11 female, 6 male) right-handed normal volunteers using a bolus intravenous injection of $^{15}O$-labelled water (half-life, 123 s) and a 40-s data acquisition[9,10]. A series of 6–10 blood flow scans were obtained in each subject (10 m interscan interval). Within this series, conditions were designed as a hierarchy of paired comparisons to allow subtractive (task minus control) data analysis (see below).

Stimuli were presented throughout data acquisition. All stimuli were frequent English nouns presented at a rate of one per second. Visually presented words appeared on a colour monitor suspended 300 mm from the subject. Auditory words were presented through hearing-aid type speakers fitted within the ears and driven by a digital tape recorder.

Four behavioural conditions formed a three-level subtractive hierarchy (Table 1). Each task state was intended to add a small number of operations to those of its subordinate (control) state[11]. In the first-level comparison, the presentation of single words without a lexical task was compared to visual fixation without word presentation. Note that no motor output or volitional lexical processing was required in this task; rather, simple

**Table 1** Paradigm design

| Subtraction | Control state | Stimulated state | Task |
|---|---|---|---|
| Sensory task | Fixation point only | Passive words | Passive sensory processing<br>Modality-specific word code |
| Output task | Passive words | Repeat words | Articulatory code<br>Motor programming<br>Motor output |
| Association Task | Repeat words | Generate uses | Semantic association<br>Selection for action |

The rationale of the three levels stepwise paradigm design is shown. At the second and third level, the control state is the stimulated state from the previous level. Some hypothesized cognitive operations are represented in the third column.

**Table 2** Sensory tasks

| Region | Coordinates (mm) Z | X | Y | Magnitude |
|---|---|---|---|---|
| Visual | | | | |
| 1. Striate cortex (L) | 10 | 6 | −72 | 2.28† |
| 2. Striate cortex (R) | 10 | −12 | −72 | 2.66† |
| 3. Extrastriate cortex (L) | 2 | 24 | −58 | 3.82‡ |
| 4. Extrastriate cortex (R) | 6 | −26 | −66 | 2.95‡ |
| 5. Inferior lateral occipital cortex (R) | −4 | −34 | −46 | 3.38‡ |
| Auditory | | | | |
| 6. Posterior superior temporal cortex (L) | 14 | 46 | −10 | 2.46† |
| 7. Temporal cortex (R) | 12 | −42 | −16 | 2.76‡ |
| 8. Anterior superior temporal cortex (L) | −2 | 42 | 10 | 3.02† |
| 9. Temporoparietal cortex (L) | 14 | 54 | −30 | 2.88‡ |
| 10. Lateral temporal cortex (R) | 8 | −62 | −12 | 3.30‡ |
| 11. Inferior anterior cingulate cortex (L) | 18 | 12 | 44 | 2.34† |

Subtraction conditions: Passive words − Fixation point. For Tables 2-4, the following conventions are used: the region is given a mnemonic anatomical name associated with the coordinates. The coordinates and magnitudes of response are determined using a three-dimensional search algorithm on the averaged subtraction image. The coordinates are in mm from a 0, 0, 0 point that is at the level of a line drawn between the anterior and posterior commissures ($z = 0$), at the mid-line of the brain ($x = 0$), and located antero-posteriorly halfway between the commissures ($y = 0$). The magnitudes are the change in blood flow in ml/(100 g × min), and the statistical significance of the points is assessed with a two-stage testing procedure. The distribution of the magnitudes of local blood-flow change is tested for outliers using an omnibus gamma-2 test. For all averaged images presented here, there are statistically significant outliers. The foci with the largest magnitude of blood-flow change are then given a $z$-score with respect to the population of all local changes within an image. All foci of change with a $P$-value $<0.03$ are reported in the tables. † $P < 0.03$, ‡ $P < 0.01$.

In general, the passive presentation subtractions identify modality-specific foci of activation, whereas the higher level subtractions activate similar regions across modalities.

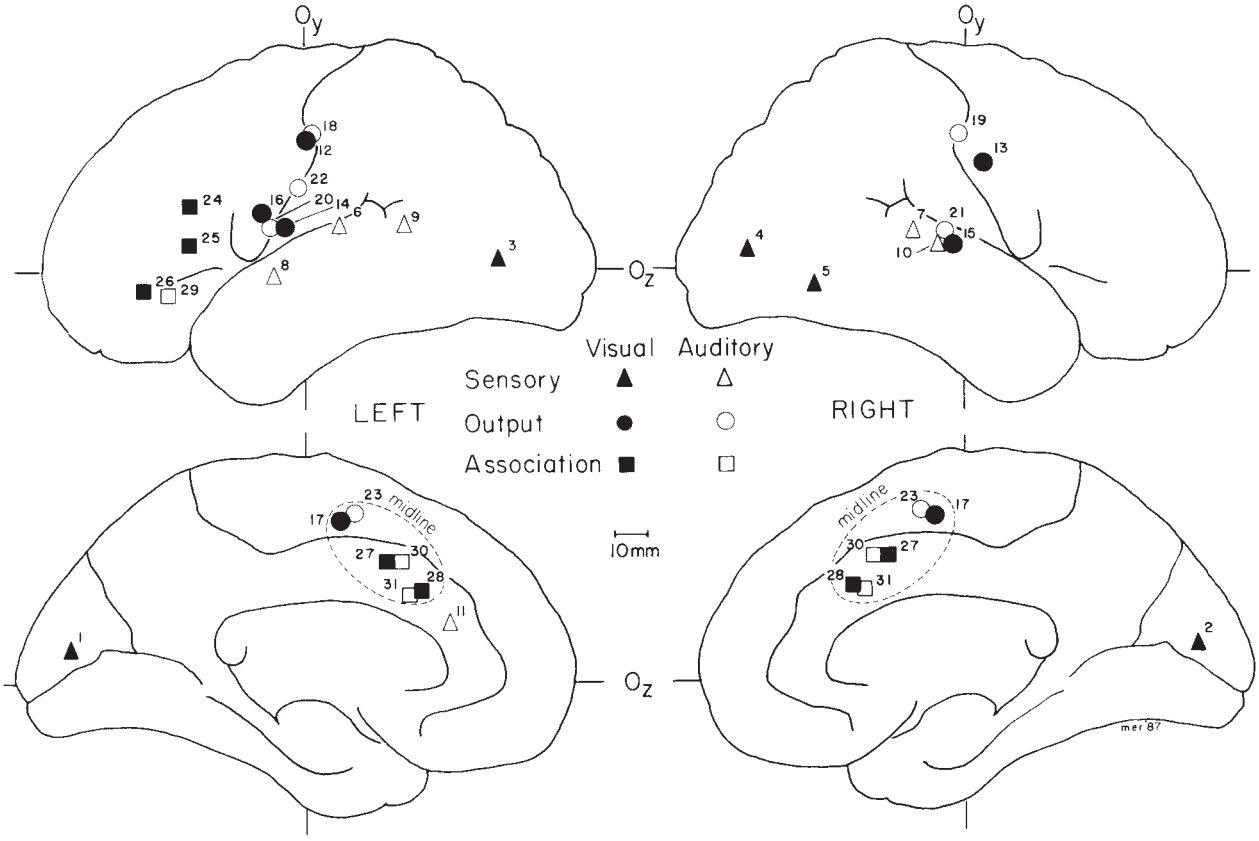


**Fig. 1** Schematic lateral (upper) and medial (lower) surface views of the left and right hemispheres with superimposed cortical activation foci. $O_y$ and $O_z$ are 0 reference planes. Each numbered symbol represents a cortical focus of activation, the number referring to Focus number in Tables 2–4. The key to the activation conditions is in the figure. Notice that for passive subtractions, there is no overlap between visual (filled triangle) and auditory (open triangle) sensory tasks. There is considerable overlap, however, between presentation modality for the association and output foci.

sensory input and involuntary word-form processing were targeted by this subtraction (sensory task). In the second-level comparison, speaking each presented word was compared with word presentation without speech. Areas involved in output coding and motor control were targeted by this comparison. In the third-level comparison, saying a use for each presented word (for example, if 'cake' was presented, to say 'eat') was compared with speaking presented words. This comparison targeted areas involved in the task of semantic processing (verb-noun association), as distinct from speech, sensory input and involuntary word-form processing (association task).

Images were analysed by paired (intrasubject) subtraction. Task-state minus control-state subtractions created images of the regional blood flow changes associated with the operations of each cognitive level. Intersubject averaging was used to increase the signal-to-noise ratio of these subtracted images[12]. Averaging required anatomical standardization of all images; this was based on a previously described stereotactic method of anatomical localization for PET images[13,14].

Statistical significance was determined by distribution analysis of the entire population (both positive and negative) of independent regional changes within each averaged subtracted image. The location and magnitude of these changes were determined using a centre-of-mass computer search algorithm[15]. Each change distribution contained both noise and task-induced responses. During averaging, task-induced responses gained in magnitude relative to image noise, becoming 'outliers' in the distribution[12]. Significant responses, then, were defined using tests for outlier detection[16]. Statistical analysis was two-tiered: first, omnibus testing (gamma-2 statistic) determined whether an image (a distribution) contained any significant responses (any outliers); then, post-hoc analysis by $Z$-score ascribed significance levels to each response within the population. All distributions reported had a gamma-2 significance level of $P < 0.05$. All cortical responses with a $Z$-score over 2.17 ($P < 0.03$) are reported.

## Lexical processing regions

Regions of activation are enumerated in Tables 2–4, and the cortical sites of activation are summarized in Fig. 1. The most striking aspect of Fig. 1 is that there are relatively few areas of activation added by each task and that these areas are clustered in a few critical parts of the cortex.

Modality-specific primary and non-primary sensory regions were activated by passive auditory or visual presentation of words (Table 2, Fig. 2*a* and *b*). No regions were activated for both auditory and visual presentation. The areas identified appear to support two different computational levels in each modality, one of passive sensory processing and a second level of modality-specific word-form processing.

For the visual modality, the main cortical activations are in the striate cortex and in a small set of prestriate areas reaching as far anterior as the temporal–occipital boundary. The primary striate responses were similar to those produced by other types of visual stimuli[17,18]. However, the regions of extrastriate occipital cortex in Table 2 have so far been activated only by the presentation of visual words. These regions may represent a network which codes for visual word form. Lesions near these regions sometimes cause pure alexia, that is, the inability to read words without other language deficits[19,20]. According to some cognitive models[1,3,21], a visual word form would be generated by a cooperative computational network including feature,

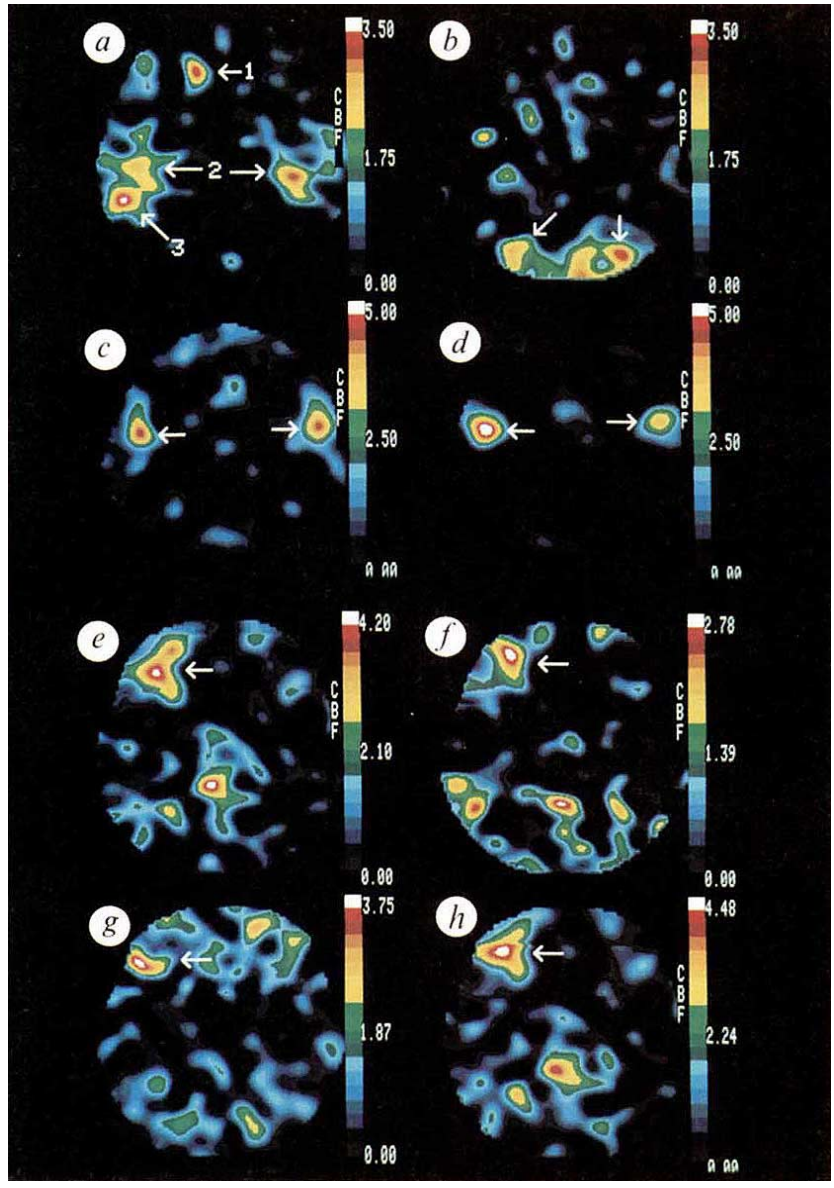


**Fig. 2** *a* and *b*, Auditory versus visual comparison. A horizontal slice through averaged subtraction image represents blood-flow change when blood-flow during fixation is subtracted from blood flow present during presentation of word stimuli at 1 Hz (sensory task). Slice in *a* and *b* is taken 1.6 cm above AC–PC line. Foci of activity present at this level include temporoparietal cortex, bilateral superior posterior temporal cortex, inferior anterior cingulate for auditory presentation, and some occipital cortical activation for visual presentation. Note the non-overlapping distributions of activity for visual and auditory presentation in *a* and *b* during passive presentation. *c* and *d*, Auditory versus visual comparison. A horizontal slice through an averaged subtraction image representing blood-flow change when blood flow during passive presentation of words is subtracted from blood flow during vocal repetition of presented words (output task). Slice is taken 4.0 cm above AC–PC line. The foci present for both auditory and visual presentation are located on rolandic cortex, just anterior and superior to regions activated by somatosensory stimulation of the lips and probably represent the mouth representation of primary motor cortex. *e* and *f*, Auditory versus visual comparison. A horizontal slice through an averaged subtraction image representing blood-flow change when blood flow during repetition of presented words is subtracted from blood flow during vocalization of an appropriate use for the presented word (such as presentation of 'cake' ... output might be 'eat') (cognitive subtraction). Slice is taken 0.8 cm below AC–PC line. Foci for both presentation modalities occur in inferior anterior frontal cortex, probably area 47 of Brodmann. Those areas of activation are strongly left-lateralized. *g* and *h*, Comparison of activation in two semantic tasks. The slice on the right (*h*) is from the same condition as *e*; *g*, the blood-flow change when the blood flow during passive presentation of words at 2.5 Hz is subtracted from blood flow during a condition where the subject is asked to monitor this string of words for members of a specific semantic category. In the semantic monitoring task, there is no motor output during the scan. Subjects are asked after the scan for a gross estimate of the percentage of target words. The similar foci of activation in these two different semantic tasks implicate this region in semantic processing. Slice is taken 0.6 cm below AC–PC line.

letter, and word levels. The multiple areas activated could represent the different levels of such a network.

For auditory processing, areas of activity were found bilaterally in primary auditory cortex, and left-lateralized in temporoparietal cortex, anterior superior temporal cortex, and inferior anterior cingulate cortex. The temporoparietal and anterior superior temporal regions have not been activated by presentation of non-word auditory stimuli[22–24]. The temporoparietal region is near the angular and supramarginal gyri, areas that have been associated in lesion studies with the phonological deficits[25,26], and is a good candidate for a phonological coding region.

Areas related to motor output and articulatory coding are activated when words are repeated aloud (Table 3). In general, similar regions were activated for visual and auditory presentation. The activated regions included primary sensorimotor mouth cortex at a location corresponding to previous descriptions of sensorimotor topography[27]. Also activated were a set of premotor structures including a midline structure (supplementary motor area, SMA) and a set of activations around the sylvian fissure. The left sylvian regions are near Broca's area, a region often viewed as specifically serving language output[7,8]. But sylvian activation was also found in the right hemisphere, and this bilateral sylvian activation was also found when subjects were instructed to simply move their mouths and tongues, arguing against specialization of this region for speech output. Small lesions confined to classically defined Broca's area most frequently cause stuttering and oral apraxia rather than full-blown Broca's aphasia[28], adding further support to the view that these regions are related to general motor, rather than language-specific output programming.

The association tasks activated two areas of cerebral cortex for both auditory and visual presentation. A left inferior frontal area was identified that almost certainly participates in processing for semantic association. The second area, anterior cingulate gyrus, appears to be part of an anterior attentional system engaged in selection for action. This localization of function was suggested by the performance of a converging experiment in which subjects monitored lists of words for members of a semantic category (such as monitoring for dangerous animals). In the semantic monitoring condition, left-frontal activation was strong and was unaffected by the number of targets in the list, supporting a semantic-processing function. Anterior-cingulate activation, however, was much stronger for lists containing many targets than for those with few, suggesting activation only when target selection was frequent. Similarly, rapid uncued move-

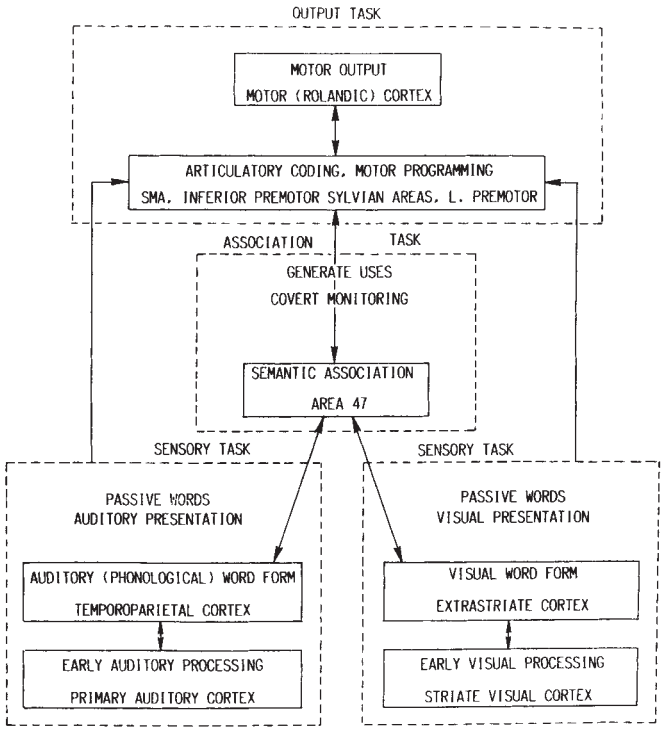


**Fig. 3** A general network relating some of the areas of activation in this study to the different levels of lexical processing. There are many alternative networks consistent with the conditions under which the areas are activated, but this arrangement represents a simple design consistent with our results, and some convergent experiments from other types of studies. The dashed boxes outline the different subtractions. The solid boxes outline possible levels of coding and associated anatomical areas of activation.

ments and imagined movements activated anterior cingulate[29], whereas monitoring very low-frequency non-linguistic visual stimuli (J. V. Pardo, P.T.F., M.E.R., unpublished observations) activated neither cingulate nor left-frontal cortex. In accord with these observations, lesions of the anterior cingulate reduced the frequency of movements and speech (akinetic mutism)[30–32], whereas left-frontal lesions produced deficits in word-fluency tests[33], and in semantic-priming tasks[34,35].

## Lexical processing models

What type of model do these results support? A serial single-route model has been widely accepted in clinical neurology[7,8]. In the serial model, access to semantics is by a phonological code, and access to output is by semantics. Thus, a visual word must be phonologically recoded (said to occur in the angular gyrus) and must establish semantic associations (Wernicke's area in the posterior temporal lobe) before output coding. Our results are more consistent with multiple-route models in concept[1–6,36–38], and are also quite inconsistent with the serial neurological model in detail.

First, there is no activation in any of our visual tasks near Wernicke's area or the angular gyrus in posterior temporal cortex. Visual information from occipital cortex appears to have access to output coding without undergoing phonological recoding in posterior temporal cortex. Second, tasks calling for semantic processing of single words activate frontal, rather than posterior, temporal regions. Third, sensory-specific information appears to have independent access to semantic codes and output codes; simple repetition (output tasks) of a presented word failed to activate the left-frontal semantic area (association tasks). A framework consistent with these results is presented in Fig. 3.

**Table 3** Output tasks

| Region | Coordinates (mm) Z | X | Y | Magnitude |
|---|---|---|---|---|
| Visual | | | | |
| 12. Mouth region, rolandic cortex (L) | 40 | 46 | 0 | 4.34‡ |
| 13. Rolandic cortex (R) | 32 | −52 | 6 | 3.46‡ |
| 14. Buried sylvian cortex (L) | 14 | 31 | 6 | 3.04† |
| 15. Lateral sylvian cortex (R) | 8 | −63 | −4 | 2.96† |
| 16. Premotor cortex (L) | 18 | 48 | 14 | 2.98† |
| 17. Supplementary motor area (SMA) | 50 | −2 | 10 | 3.36† |
| Auditory | | | | |
| 18. Mouth region, rolandic cortex (L) | 42 | 46 | −2 | 3.64‡ |
| 19. Rolandic cortex (R) | 40 | −56 | 2 | 3.78‡ |
| 20. Buried sylvian cortex (L) | 14 | 34 | 10 | 3.17† |
| 21. Lateral sylvian cortex (R) | 12 | −62 | −7 | 3.22‡ |
| 22. Premotor cortex (L) | 26 | 52 | 2 | 3.06† |
| 23. SMA | 52 | 2 | 14 | 2.80† |

Subtraction conditions: Repeat words − Passive visual words. See Table 2 legend for details of conventions used.

**Table 4** Association tasks

| Region | Coordinates (mm) Z | X | Y | Magnitude |
|---|---|---|---|---|
| Visual | | | | |
| 24. Dorsolateral prefrontal cortex (L) | 20 | 44 | 36 | 2.98‡ |
| 25. Lateral prefrontal cortex (L) | 8 | 38 | 36 | 2.96‡ |
| 26. Inferior prefrontal Cortex (L) | −6 | −28 | 50 | 2.26† |
| 27. Anterior cingulate | 38 | −6 | 24 | 3.12‡ |
| 28. Inferior anterior cingulate | 28 | −2 | 34 | 2.76‡ |
| Auditory | | | | |
| 29. Inferior prefrontal cortex (L) | −6 | 33 | 43 | 3.10‡ |
| 30. Anterior cingulate | 38 | 7 | 28 | 3.28‡ |
| 31. Inferior anterior cingulate | 28 | 11 | 31 | 3.04‡ |

Subtraction conditions: Generate words − Repeat visual words. See Table 2 legend for details of conventions used.

The combination of cognitive and neurobiological approaches, of which this study is an example, has given us information about the functional anatomy of perception, attention, motor control, and language. As these endeavours proceed, solutions to the problem of mind-brain interaction that have intrigued us for so long should be illuminated.

This work was supported in part by the Office of Naval Research the National Institute of Health, and by the McDonnell Center for Higher Brain Function and the MacArthur Foundation.

Received 6 October 1987; accepted 5 January 1988.

1. LaBerge, D. & Samuels, J. *Cognitive Psychol.* **6**, 293-323 (1974).
2. Rumelhart, D. E. & McClelland, J. L. *Psychol. Rev.* **89**, 60-94 (1982).
3. Rumelhart, D. E. & McClelland, J. L. *Parallel Distributed Processing* Vols 1 and 2 (MIT, Cambridge, 1986).
4. Carr, T. H. & Pollatsek, A. *Reading Research* Vol. 5, 1-82 (Academic, New York, 1985).
5. Posner, M. I. in *Chronometric Explorations of Mind* (Posner, M. I. & Marin, O. S. M.) (Erlbaum, Englewood Height, N.J., 1978).
6. Coltheart, M. *Attention and Performance XI* (Erlbaum, Hilldale, N.J., 1985).

7. Geschwind, N. *Brain* **88,** 237–294, 585–644 (1965).
8. Geschwind, N. *Scient. Am.* **241,** 158–168 (1979).
9. Herscovitch, P., Markham, J. & Raichle, M. E. *J. Nucl. Med.* **24,** 782–789 (1983).
10. Raichle, M. E., Martin, W. R. W., Herscovitch, P., Mintun, M. A. & Markham, J. *J. Nucl. Med.* **24,** 790–798 (1983).
11. Sternberg, S. *Acta Psychol.* **30,** 276–315 (1969).
12. Fox, P. T., Mintun, M. A. & Raichle, M. E. *J. cerebral Blood Flow Metab.* (in the press).
13. Fox, P. T., Perlmutter, J. S. & Raichle, M. E. *J. Comp. Assist. Tomogr.* **9,** 141–153 (1985).
14. Tailarach, J. *et al. Atlas d'Anatomie Stereotaxique due Telencephale* (Masson, Cie., Park, 1967).
15. Mintun, M. A., Fox, P. T. & Raichle, M. E. *Soc. Neurosci. Abstr.* **13,** 850 (1987).
16. Snedecor, G. W. & Corcoran, W. G. *Statistical Methods* (Iowa University Press, Iowa City, 1980).
17. Fox, P. T. *et al. Nature* **323,** 806–809 (1986).
18. Fox, P. T., Miezin, F. M., Allman, J. M., Van Essen, D. C. & Raichle, M. E. *J. Neurosci.* **7,** 913–922 (1987).
19. Damasio, A. R. & Damasio, H. *Neurology* **33,** 1573–1583 (1983).
20. Henderson, V. W. *Brain Lang.* **29,** 119–133 (1986).
21. McClelland, J. L. & Rumelhart, D. E. *Psychol. Rev.* **88,** 375–407 (1981).
22. Lauter, J., Herscovitch, P., Formby, C. & Raichle, M. E. *Hearing Res.* **20,** 199–205 (1985).
23. Mazziota, J. C., Phelps, M. E., Carson, R. E. & Kuhl, D. E. *Neurology* **32,** 921–937 (1982).
24. Roland, P., Larson, B., Lassen, N. A. & Skinhoj, E. *J. Neurophysiol.* **43,** 118–136 (1980).
25. Roeltgen, D. P., Sevush, S. & Heilman, K. M. *Neurology* **33,** 755–765 (1983).
26. Shallice, T. *Brain* **104,** 413–429 (1981).
27. Fox, P. T. & Raichle, M. E. *Proc. natn. Acad. Sci. U.S.A.* **83,** 1140–1144 (1986).
28. Mohr, J. P. *et al. Neurology* **28,** 311–324 (1978).
29. Fox, P. T., Pardo, J. V., Petersen, S. E. & Raichle, M. E. *Soc. Neurosci. Abstr.* **13,** 1433 (1987).
30. Masdau, J. C., Schoene, W. C. & Funkenstein, H. *Neurology* **28,** 1220–1223 (1978).
31. Barris, R. W. & Schuman, H. R. *Neurology* **3,** 44–52 (1953).
32. Nielsen, J. M. & Jacobs, L. L. *Bull. L.A. Neurol. Soc.* **16,** 231–234 (1951).
33. Benton, A. L. *Neuropsychologia* **6,** 53–60 (1968).
34. Milberg, W. & Blumstein, S. E. *Brain Lang.* **14,** 371–385 (1981).
35. Milberg, W., Blumstein, S. E. & Dworetzky, B. *Brain Lang.* **31,** 138–150 (1987).
36. Humphreys, G. W. & Evett, E. J. *Behav. Brain Sci.* **8,** 689–740 (1985).
37. Shallice, T., McLeod, P. & Lewis, K. *Q. J. exp. Psychol.* **37A,** 507–532 (1985).
38. Coltheart, M., Davelaar, E., Jonasson, J. & Besner, D. in *Attention and Performance VI* (ed. Dornic, S.) (Academic, New York, 1977).

# LETTERS TO NATURE

## ESO400-G43, a forming galaxy?

**Nils Bergvall* & Steven Jörsäter†**

* Astronomiska observatoriet, Box 515, S-751 20 Uppsala, Sweden
† European Southern Observatory, Karl-Schwarzschild-Strasse 2, D-8046 Garching bei München, FRG and Stockholms Observatorium, S-133 00 Saltsjöbaden, Sweden

**Blue compact galaxies (BCGs) are characterized by their compact appearance and very blue colours[1,2] indicative of a high star-formation rate. The metal abundances are low, suggesting that the present rate of star formation cannot have lasted for very long[3] (unless the gas is being replenished). These galaxies are thus either truly young or their star formation takes place in short bursts[3,4]. ESO400-G43 (=2034−356) is one of the brightest and largest BCGs known. Observations in the 21-cm line with the Very Large Array (VLA) of the National Radio Astronomy Observatory reveal a massive ($5\times10^9\ M_\odot$) slowly rotating H I halo. Optical observations obtained at the European Southern Observatory (ESO) show that the morphology and spectral properties are consistent with a predominantly young stellar population and an extremely low mass to light ratio ($M/L_B=0.1$). The luminous stars seem to be concentrated in a rapidly spinning central disk. Dark matter is dominating the mass at large radii.**

We have obtained charge coupled device (CCD) images of ESO400-G43 with the ESO 2.2-m telescope in the Johnson U,B,V and the *i* bands (ref. 5). An irregular appearance with numerous hot spots that show up also in the red is seen (Fig. 1). Image Dissector Scanner (IDS) spectra were obtained with the ESO 3.6-m telescope in 1980 and 1982. The spectra were corrected for IDS nonlinearity[6]. CCD spectra were obtained in 1982 and 1985 with the ESO 3.6-m telescope. The observations were corrected for extinction based on an averaged $H\alpha/H\beta$ ratio across the galaxy after correction for underlying absorption lines (the correction is ~15% for $H\beta$); the extinction is moderate ($A_V\approx0.6$). The strength of the Balmer absorption lines were obtained from the spectrophotometric model discussed below.

The spectra are dominated by strong emission lines typical of H II regions heated by hot, massive stars. An electron temperature of $T_e\approx12{,}000$ K was determined from the [O III] $\lambda4{,}363/\lambda\lambda\ 4{,}959+5{,}007$ line ratio. We derive a gas metallicity using the ratios between the $H\beta$ and [N II], [O II] and [O III] lines of $Z\approx1/8\ Z_\odot$. The blue-ultraviolet excess is large ($U-B=-0.60$; K. Olofsson, personal communication) and it is one of the intrinsically brightest objects of its type ($M_V=-20.1$). ESO400-G43 was detected by IRAS (Infrared Astronomy Satellite) at 60 μm and 100 μm.

We observed ESO400-G43 in the 21-cm H I line with the VLA in its B/C hybrid configuration in July 1985. The H I observations were made using 25 antennae with an effective channel width of 97.7 kHz corresponding to 21.0 km s$^{-1}$ and a total number of 31 channels. The total integration time on source was 8 hours. The interferometric data were edited in the usual way and were further processed using the Astronomical Image Processing System (AIPS). The H I emission of E400-G43 was detected in 9 channel maps in the heliocentric velocity range 5,745–5,913 km s$^{-1}$ (optically defined).

The continuum-subtracted (using line-free channels) cleaned and smoothed (to a beamsize of 20″×20″) channel maps are shown in Fig. 2. The maps were subsequently blanked using a smoothed template in the spatial plane and afterwards interactively using the AIPS task BLANK. The resulting total H I map is shown in Fig. 3*a* and the derived velocity field in Fig. 3*b*. The total H I flux is 7.8 Jy km s$^{-1}$, corresponding to a total H I mass of $1.1\times10^{10}\ M_\odot$.

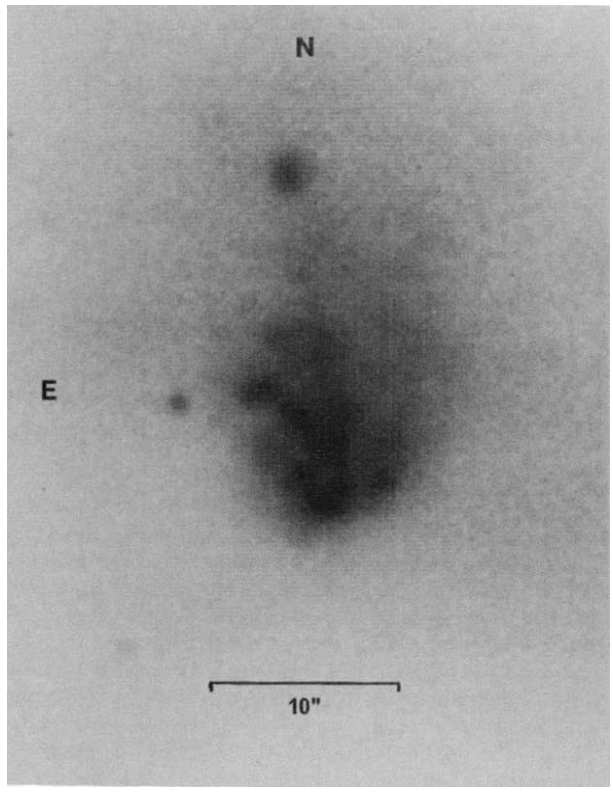


**Fig. 1** A CCD image of ESO400-G43 obtained through an *i* filter (~8,200 Å) with the 2.2-m telescope at ESO, La Silla, Chile. The distance is 77 Mpc assuming Hubble's constant is 75 km s$^{-1}$ Mpc$^{-1}$ (1 arc s ≈380 pc).